



## Characterization and catalytic activity of CuFeZSM-5 catalysts for oxidative degradation of Rhodamine 6G in aqueous solutions

M. Dükkancı<sup>a</sup>, G. Gündüz<sup>a,\*</sup>, S. Yılmaz<sup>b</sup>, Y.C. Yaman<sup>a</sup>, R.V. Prikhod'ko<sup>c</sup>, I.V. Stolyarova<sup>c</sup>

<sup>a</sup> Ege University, Chemical Engineering Department, 35100 Bornova, Izmir, Turkey

<sup>b</sup> Izmir Institute of Technology, Chemical Engineering Department, Gülbahçe Village, 35437 Urla, Izmir, Turkey

<sup>c</sup> Dumanski Institute of Colloid and Water Chemistry, National Academy of Sciences of Ukraine, Kiev, Ukraine

### ARTICLE INFO

#### Article history:

Received 11 November 2009

Received in revised form 25 December 2009

Accepted 7 January 2010

Available online 14 January 2010

#### Keywords:

CuFeZSM-5 zeolite

Ion exchange

Hydrothermal synthesis

Rhodamine 6G

Hydrogen peroxide

### ABSTRACT

This study presents an evaluation of the catalytic performances of Fe and Cu containing ZSM-5 zeolites for oxidation of Rhodamine 6G. Fe and Cu were loaded by ion exchange or through hydrothermal synthesis. The catalytic process was carried out in an aqueous solution using H<sub>2</sub>O<sub>2</sub> as an oxidant. The catalyst prepared by hydrothermal synthesis showed the highest activity (100% decolorization, 59.1% aromatic degradation and 51.8% TOC removal at initial pH of 3.5). This catalyst was stable against leaching even at low pH. The change in activity of the catalysts prepared was attributed to incorporation of the Fe and Cu species with ZSM-5. Fe and Cu were in structural locations – in the framework – in the catalyst prepared by hydrothermal synthesis while there were extraframework cations or species in catalysts prepared by ion exchange. Incorporation of Cu into FeZSM-5 increased its catalytic activity.

© 2010 Elsevier B.V. All rights reserved.

### 1. Introduction

Waste water from different chemical processes such as petrochemical units, dye and dye intermediate manufacturing industries and textile units contain toxic organic compounds. Their discharge into the environment pollutes the water. These compounds are hazardous to microorganisms as well as having carcinogenic effects for human. Thus, during the last decade abatement of these compounds in wastewater has been investigated. Wet air oxidation is a common technology for reducing total organic carbon (TOC) in industrial waste water [1]. But the high reaction temperature required during the oxidation allows economic operation only when the heat of reaction released during the oxidation is enough.

Among the new technologies (advanced oxidation), the catalytic wet air oxidation (CWAO) using air or oxygen as oxidant achieves high conversions, but unfortunately high temperatures are needed for this process too [2]. The use of H<sub>2</sub>O<sub>2</sub> allows to perform oxidation reaction at ambient conditions, decreasing the investment costs. These novel destruction techniques are based on the generation of hydroxyl radicals, which are able to mineralize the toxic chemicals in waste water. For the generation of OH<sup>\*</sup> radicals from H<sub>2</sub>O<sub>2</sub> and minimization of the side reaction of

decomposition to water, catalytic activation is needed. The oxidation using Fenton's reagent, a powerful source of oxidative HO<sup>\*</sup> radicals generated from H<sub>2</sub>O<sub>2</sub> in the presence of Fe<sup>2+</sup> ions, has proved to be a promising and attractive treatment method for the effective destruction of a large number of toxic pollutants [3]. The generated HO<sup>\*</sup> radicals are highly oxidative, non-selective and able to decompose many organic compounds including dyes. Fenton's reagent has been one of the most common homogeneous systems proposed for treatment of textile waste waters [4–8].

Amount of iron used in homogeneous Fenton process is above European Union limits. Thus, wastewater cannot be discharged with the Fe used. In addition, treatment of the sludge containing iron is not economic and it requires manpower and chemicals. And also strict control of pH around 2–3 is required. These drawbacks can be overcome by using heterogeneous Fenton-type catalysts. Some attempts have been made to develop heterogeneous catalysts by incorporating Fe ions or Fe oxides into porous supports [9–14]. Recently high catalytic activity of iron containing zeolites [15] and copper containing pillared clays [16] for phenol oxidation have been reported. Fe-exchanged Y zeolite was used for wet peroxide oxidation of reactive azo dye Procion Marine H-EXL [4]. The catalyst allowed almost total elimination of the dye and significant removal of COD and TOC. FeZSM-5 prepared by ion exchange was tested in wet oxidation with hydrogen peroxide of diluted formic, acetic and propionic acids [1]. The results indicated that heterogeneous catalyst was very active at a wide range of pH in comparison to the homogeneous Fe<sup>3+</sup> catalysts.

\* Corresponding author. Tel.: +90 2323884000/2292; fax: +90 2323887776.  
E-mail address: [gonul.gunduz@ege.edu.tr](mailto:gonul.gunduz@ege.edu.tr) (G. Gündüz).

Copper containing catalysts such as Al–Cu catalyst supported on pillared clay and CuO catalyst supported on  $\gamma$ -Al<sub>2</sub>O<sub>3</sub> showed high catalytic activity during oxidation of phenol dissolved in water [17]. Isolated Cu<sup>2+</sup> sites grafted to Al-MCM-41 also gave relatively high catalytic activity in ethane oxidation [18]. On the other hand, copper exchanged zeolites such as CuZSM-5 have been widely studied for selective catalytic reduction of NO<sub>x</sub> to N<sub>2</sub> with ammonia [19–21].

The aim of the present study is to investigate Fe and Cu containing ZSM-5 zeolites, Fe and Cu loaded by ion exchange or by hydrothermal synthesis, for wet peroxide oxidation of Rhodamine 6G which is an important dye used in textile industry.

## 2. Experimental

### 2.1. Materials

ZSM-5 (AlSi-Penta, Si/Al = 22, sodium form) used in catalyst preparation by ion exchange was obtained from VAW Company, Germany. The reactive azo dye Rhodamine 6G was obtained from Sigma–Aldrich and used without further purification. The absorption spectra of Rhodamine 6G is characterized by three main bands, one in the visible region ( $\lambda_{\text{max}} = 523$  nm) which is responsible for the chromophoric components (for the color of dye arising from aromatic rings connected by azo groups) and the others in the UV region ( $\lambda_{\text{max}} = 246$  nm and  $\lambda_{\text{max}} = 275$  nm) which represent the absorption of benzene-like and naphthalene-like structures in the molecule, respectively [9]. Rhodamine 6G is called R6G, Rh6G, C.I. Pigment Red 81, C.I. Pigment Red 169, C.I. 45160 where C.I. is the color index. The hydrogen peroxide solution (35%) of analytical grade was obtained from Merck. Aqueous solutions containing 0.1 g/dm<sup>3</sup> azo dye were prepared with deionized water from a Millipore Direct Q purification unit.

Fig. 1 presents the chemical structure of Rhodamine 6G (R6G) (a) and UV–vis absorption spectra of aqueous solutions of Rhodamine 6G (b).

### 2.2. Catalyst preparation

Ion exchange (IE) and hydrothermal synthesis (HT) were used for catalyst preparation. For ion-exchange, method used by Schwidder et al. [22] was applied with little modifications. For this purpose, 5 g of parent ZSM-5 (AlSi-Penta, VAW) zeolite, 1.825 g of Fe powder (Riedel-de Haen AG) and 500 cm<sup>3</sup> of deionized water were charged into a double-necked flask equipped

with a gas-inlet tube and a magnetic stirrer. After the flask was flushed with nitrogen for 3 min, 4.14 cm<sup>3</sup> of concentrated hydrochloric acid (in mass % of 37, J.T. Baker) was slowly added to the mixture. After the liquid was stirred under nitrogen atmosphere for 5 days it was removed, and the prepared FeZSM-5 sample which was in reddish brown color was washed with deionized water. Washing was repeated until no Cl<sup>−</sup> was detected in the washing water. Part of this catalyst was dried at room temperature and calcined. For calcination, catalyst was first heated to 423 K at a heating rate of 353 K/min and kept there for 15 min and then it was heated to 873 K at a rate of 323 K/min and kept at that temperature for 2 h. The color of the sample did not change after calcination at 873 K. This catalyst was named as IE-FeZSM-5. The other part of uncalcined FeZSM-5 catalyst was first dried at 353 K for 1 h and then 398 K for 30 min and then subjected to ion exchange of copper [19]. For this purpose 2.72 g dried sample was mixed with 72.5 cm<sup>3</sup> of 11 mM Cu(CH<sub>3</sub>COO)<sub>2</sub>(Cu(Ac)<sub>2</sub>) (Merck) in an erlenmeyer. The solution pH was measured as 5.1 and NH<sub>3</sub> (>65%, Uparc) was added till pH was 8 and it was stirred for 14 h. After that the catalyst was filtered, washed and left at room temperature for drying. Then it was kept at 353 K for 1 h and at 398 K for 1/2 h. The resultant material was called as IE-CuFeZSM-5.

For the hydrothermal synthesis, the method given by Szostak et al. [23] was applied to prepare HT-FeZSM-5 sample. Same method was used with copper addition for HT-CuFeZSM-5. For this purpose, 1.872 g of Fe(NO<sub>3</sub>)<sub>3</sub>·9H<sub>2</sub>O (>99.99%, Sigma) was dissolved in 22.5 g H<sub>2</sub>O. The solution was acidified with 3.75 g H<sub>2</sub>SO<sub>4</sub> (95–98%, Merck). 50 g Na<sub>2</sub>SiO<sub>3</sub>·5H<sub>2</sub>O (97%, Sigma) dissolved in 50 g H<sub>2</sub>O and 0.28 g Cu(Ac)<sub>2</sub> dissolved in 2.5 g water were added to the first solution. Immediate formation of a pale yellow gel was observed. To the gel 6 g tetrapropylammonium bromide (TPABr) (>98%, Fluka) in 12.5 g H<sub>2</sub>O was added and then its pH was reduced to 9.40 by addition of H<sub>2</sub>SO<sub>4</sub> solution. This gel was kept in an autoclave at 443 K for 3 days under autogeneous pressure. The resulting white solid was filtered, washed and dried at 373 K for 12 h. For calcination, the dried powder was heated to 423 K at a heating rate of 353 K/min and kept there for 15 min, then heated to 873 K at a heating rate of 323 K/min and kept at this temperature for 2 h. This catalyst was named as HT-CuFeZSM-5.

### 2.3. Catalyst characterization

Powder X-ray diffraction (XRD) patterns of the solids were recorded in the range of 5–70° by Philips X'Pert Pro with Cu K $\alpha$

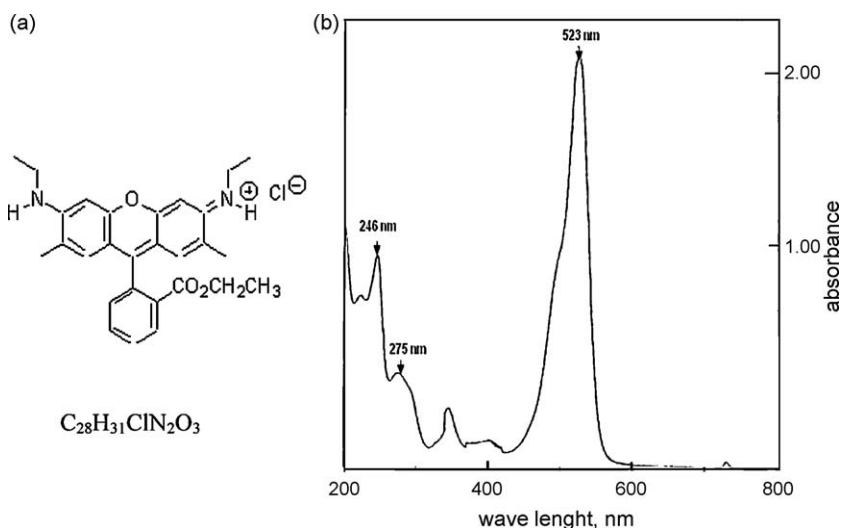


Fig. 1. Chemical structure of Rhodamine 6G (R6G) (a) and UV–vis absorption spectra of aqueous solutions of Rhodamine 6G (b).

radiation to determine the crystalline structure of the samples. Morphological properties were analyzed by scanning electron microscopy (Philips SFEG 30S SEM). The catalyst samples were analyzed by Energy Dispersive X-Ray (EDX) system attached to SEM. Nitrogen adsorption and desorption isotherms at 77 K were measured using Micromeritics ASAP 2010 equipment after degassing the dried samples at 573 K for 24 h under  $5 \mu\text{m Hg}$  vacuum. FT-infrared spectra were recorded in the  $1700\text{--}400 \text{ cm}^{-1}$  with a Shimadzu FT-IR 8201 spectrometer using KBr pellet technique. A typical pellet containing 1 wt.% of sample was prepared by mixing 2 mg sample with 200 mg KBr.

Temperature-programmed reduction (TPR) was carried out using Micromeritics AutoChem II Chemisorption Analyzer. The catalyst samples were outgassed at 773 K for 1 h and then cooled to 323 K under He flow. TPR profiles were registered while heating the samples from room temperature to 873 K by 278 K/min heating rate under flow of 5%  $\text{H}_2/\text{He}$  mixture ( $20 \text{ cm}^3/\text{min}$ ). The sample was then cooled to 323 K under 5%  $\text{H}_2/\text{He}$ . After that the flow was switched to He and the samples were cooled.

#### 2.4. Catalytic activity tests

The oxidative degradation of Rhodamine 6G was performed under isothermal conditions in a temperature-controlled shaded glass batch reactor equipped with a mechanic stirrer and a pH electrode. In a typical run,  $150 \text{ cm}^3$  of aqueous dye solution ( $0.1 \text{ g}/\text{dm}^3$ ) was placed into the reactor and the temperature was adjusted to 323 K. When the temperature reached to 323 K, pH of the solution was measured and 0.15 g of catalyst ( $1 \text{ g}/\text{dm}^3$ ) was introduced into the solution under continuous stirring. After stabilization of the temperature at 323 K, pH of the solution was again measured and the solution was analyzed in order to determine whether the dye is adsorbed by the catalyst. Then a solution of 35%  $\text{H}_2\text{O}_2$  ( $40 \text{ mmol H}_2\text{O}_2/150 \text{ cm}^3$  solution namely 0.267 M) was added into the dye solution. This time was recorded as the starting time of the reaction. After the addition of  $\text{H}_2\text{O}_2$ , pH of the solution was again measured. For the experiments with initial pH of 3–4, pH was regulated by addition of  $\text{H}_2\text{SO}_4$  into the dye solution. The samples taken periodically at every 15 min were diluted in 1:10 ratio. After centrifugation for 0.5 h to separate the catalyst, the samples were analyzed with UV spectrophotometer (Jasco 7800 UV/Vis).

The decrease of the intensity of the band at 523 nm was used as a measure of decolorization degree and the decrease of the intensity of the band at 275 nm was taken as a measure of degradation degree. The decrease in the intensity of the latter band is attributed to the formation of intermediates resulting from the degradation of the azo dye, which still contain benzoic and naphthalene type rings [1].

In addition to these measurements, total organic carbon (TOC) removal was determined using a TOC Shimadzu Vcph spectrophotometer for each run after a reaction time of 2 h for the evaluation of the mineralization of R6G dye. TOC was calculated as the difference between the total carbon (TC) and inorganic carbon (IC) in the liquid sample.

### 3. Results and discussion

#### 3.1. X-ray diffraction studies

XRD patterns of CuFeZSM-5 samples are displayed in Fig. 2 together with the parent ZSM-5 zeolite used in ion exchange. All samples exhibited the typical diffractograms of the MFI framework ( $2\theta = 7\text{--}9^\circ$  and  $23\text{--}25^\circ$ ) which emphasized high dispersion of Cu and Fe ions in compensating positions inside zeolites [24–32]. The course of the baseline indicated that no-impurity phase was

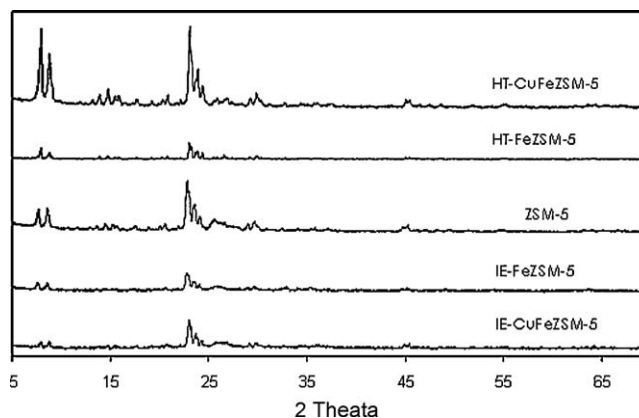


Fig. 2. X-ray diffraction patterns of prepared CuFeZSM-5 and FeZSM-5 samples and parent ZSM-5 zeolite.

observed. The decrease in the peak intensities in the IE-CuFeZSM-5 and IE-FeZSM-5 samples can be attributed to the enhanced absorption of X-ray due to Fe and Cu cations [22,30,33]. On the other hand, the decrease in peak intensities is in correlation with the decrease in crystal size of zeolite as a result of the acid processing step and with the increase in the quantities of nonuniform zones connected with washing away Al from the skeleton of zeolite and also with the formation of X-ray amorphous CuO phases on the zeolite surface.

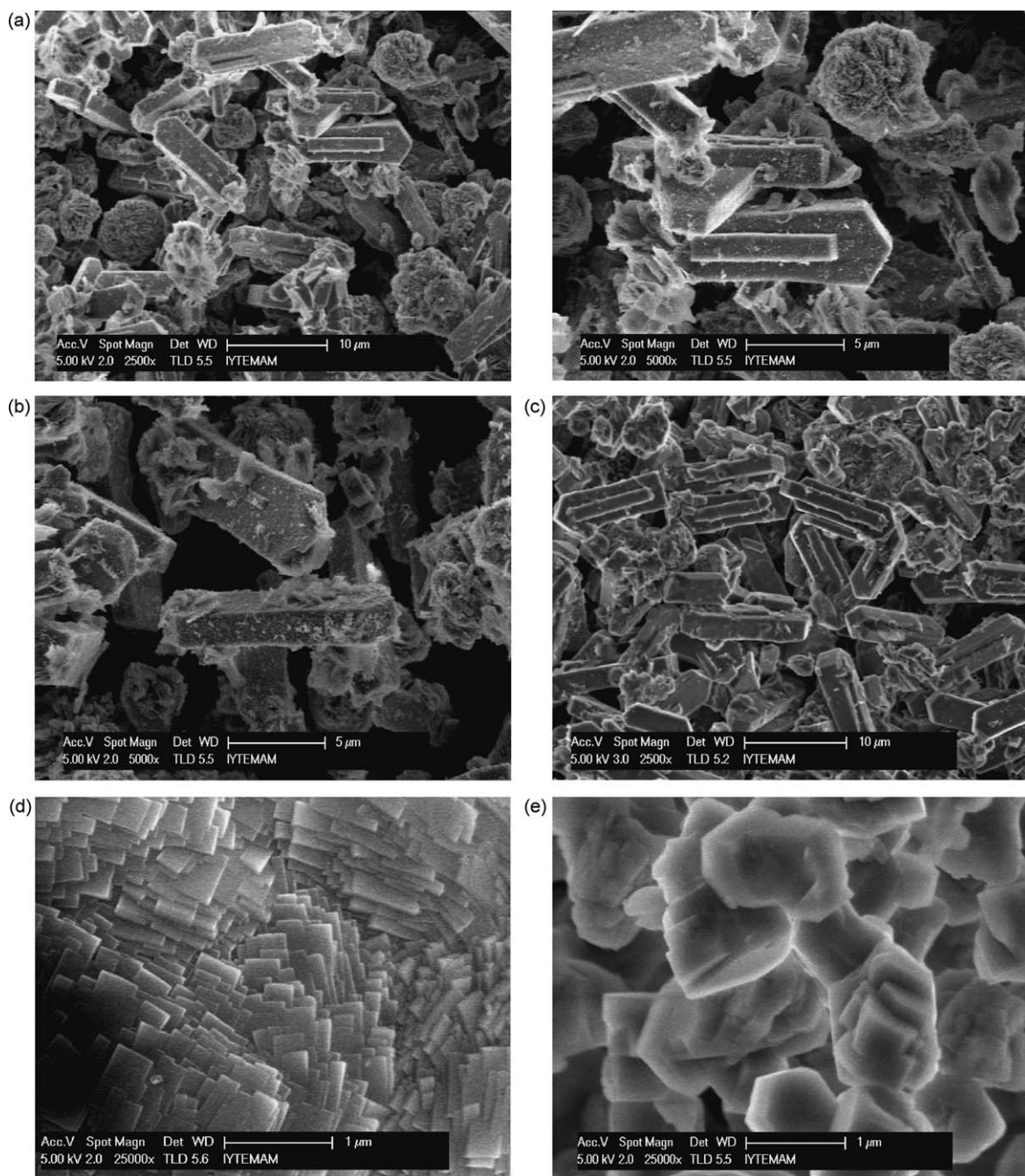
#### 3.2. SEM studies

Fig. 3 indicates the morphology of parent ZSM-5, IE-CuFeZSM-5, IE-FeZSM-5, HT-FeZSM-5 and HT-CuFeZSM-5. SEM image of the sample prepared by ion-exchange method, IE-CuFeZSM-5, depicted that the crystallites in this sample were as coffin-like shape [13] with a length of  $10 \mu\text{m}$  (Fig. 3a). For this catalyst, the increase in number of amorphous inclusions is precisely visible. When the SEM images of IE-CuFeZSM-5 and IE-FeZSM-5 samples were compared with that of parent ZSM-5 zeolite, incorporation of iron and copper in ZSM-5 structure could be clearly observed (Fig. 3, comparison of a and b with c). Extraframework iron and copper were present in these samples.

The SEM image of HT-CuFeZSM-5 sample revealed that the sample prepared by hydrothermal synthesis method was consisting of platelets with no evidence for the presence of copper and iron ions (Fig. 3d). This manifested the high dispersion of these ions in zeolite as evoked by XRD data. SEM image of HT-FeZSM-5 presents grains identical with the size of  $1 \mu\text{m}$ . The absence of a secondary iron phase indicates framework iron is present in the sample (Fig. 3e).

#### 3.3. FTIR measurements

IR spectra of the zeolite vibration modes and the corresponding Fe and Cu containing ones were depicted in Fig. 4 in the range of  $400\text{--}1700 \text{ cm}^{-1}$ . All spectra showed that bands at 445, 550, 800, 1100, 1225 and  $1650 \text{ cm}^{-1}$  which are assigned to different vibrations of tetrahedral and framework structure of ZSM-5 zeolite associated with minor changes as a result of Fe and Cu incorporation. The bands at about 1100 and  $445 \text{ cm}^{-1}$  are due to the internal vibrations of (Si, Al)  $\text{O}_4$  tetrahedra of ZSM-5, whereas the bands at 1225 and  $800 \text{ cm}^{-1}$  are due to vibrations related to external linkages between tetrahedral and hence sensitive to framework structure. The band at  $550 \text{ cm}^{-1}$  has been assigned to the five membered ring of the pentasil zeolite structure [22,23,25,28,33]. The band appearing at around  $650 \text{ cm}^{-1}$  was



**Fig. 3.** SEM images of prepared samples: IE-CuFeZSM-5 (a), IE-FeZSM-5 (b), ZSM-5 (c), HT-CuFeZSM-5 (d), HT-FeZSM-5 (e).

related to CuO vibration mode and  $-(\text{Si}-\text{O}-\text{Fe})_n$  – symmetric stretching vibration band [23,33,34].

### 3.4. Nitrogen adsorption measurements

The surface characteristics of samples including BET-surface area ( $S_{\text{BET}}$ ), total pore volume ( $V_p$ ), average pore diameter ( $d_{\text{ave}}$ ), are given in Table 1. Incorporation of copper (by ion-exchange method) into iron containing ZSM-5 decreased the BET-surface area from 507.7 to 294.0  $\text{m}^2/\text{g}$ , which precisely specifies the presence of an additional phase. This could be due to the occurrence of some copper species inside zeolite pores and thus blocking them. The catalyst sample synthesized by hydrothermal method, HT-CuFeZSM-5, had greater average pore diameter (3.82 nm) than those (2.44 nm) prepared by ion-exchange method.

Nitrogen adsorption isotherms of the samples, Fig. 5, were of type I with the exception of the isotherms of samples HT-CuFeZSM-5 and IE-FeZSM-5 (those are of type II). It is well known that isotherm of type I corresponds to a complete monolayer formation, typical for microporous materials and the isotherm of type II to multilayer formation which is the case of physical adsorption.

### 3.5. Chemical composition of the ZSM-5 samples

The content of iron and copper in the zeolite samples was determined by energy dispersive X-ray (EDX) analysis. The average of analysis of eight fields was taken in EDX analysis. As seen from Table 1, parent ZSM-5 includes iron as impurity. More iron and copper were loaded by ion exchange compared to hydrothermal method. The amounts of iron and copper loaded by ion exchange

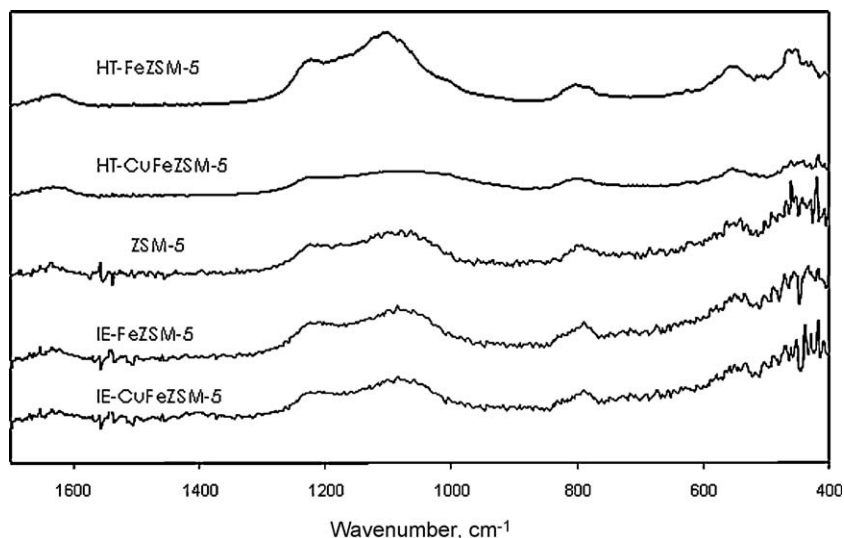


Fig. 4. FTIR spectra of the parent ZSM-5 and CuFeZSM-5 and FeZSM-5 samples prepared.

Table 1

Surface characteristics and physicochemical properties of parent ZSM-5 and iron and copper containing ZSM-5 zeolites prepared.

Sample	$S_{\text{BET}}$ (m <sup>2</sup> /g)	$V_p$ (cm <sup>3</sup> /g)	$d_{\text{ave}}^a$ (nm)	Si/Al	wt.%Fe	wt.%Cu	Si/Fe	Si/Cu
ZSM-5	227.1	0.121	2.13	22.18	0.64	–	161.90	No copper
IE-FeZSM-5	507.7	0.280	2.52	19.74	18.00	–	4.60	No copper
IE-CuFeZSM-5	294.0	0.160	2.44	20.26	19.54	2.53	4.42	38.81
HT-CuFeZSM-5	390.0	0.254	3.82	No aluminum	2.89	0.93	35.76	125.29
HT-FeZSM-5	344.4	0.192	2.51	No aluminum	3.42	–	30.31	No copper

<sup>a</sup> By Horvath Kawazoe method.

are about sevenfold and threefold of those in the sample prepared by hydrothermal method, respectively.

### 3.6. Reduction of transition metals

The catalysts were also characterized by the temperature-programmed reduction with hydrogen ( $H_2$ -TPR), which can be used to determine the structural localization and dispersity of oxide clusters of iron and the reversibility of its reduction–oxidation. The  $H_2$ -TPR curves of IE-FeZSM-5 and IE-CuFeZSM-5 and HT-CuFeZSM-5 are given in Fig. 6. IE-FeZSM-5 and IE-CuFeZSM-5 catalysts had one major  $H_2$  consumption peak at 631 and 708 K,

respectively. At higher temperatures much less  $H_2$  consumption was observed. The amount of  $H_2$  uptake increased with loading of Cu in the catalysts prepared by ion exchange. The reduction at low temperatures was attributed to the reduction of out-of-framework compounds of the  $Fe_xO_y$  and  $(Fe_xO_y)_n$  types [24], whereas the higher temperature peak corresponded to reduction of structural ions of iron(III). However, HT-CuFeZSM-5 showed much less  $H_2$  consumption. A low temperature peak was observed at 559 K. This implied that iron and copper species were in the framework of HT-CuFeZSM-5. The diverse nature and composition of active centers and the surface chemistry may strongly affect the behavior of the catalysts under study.

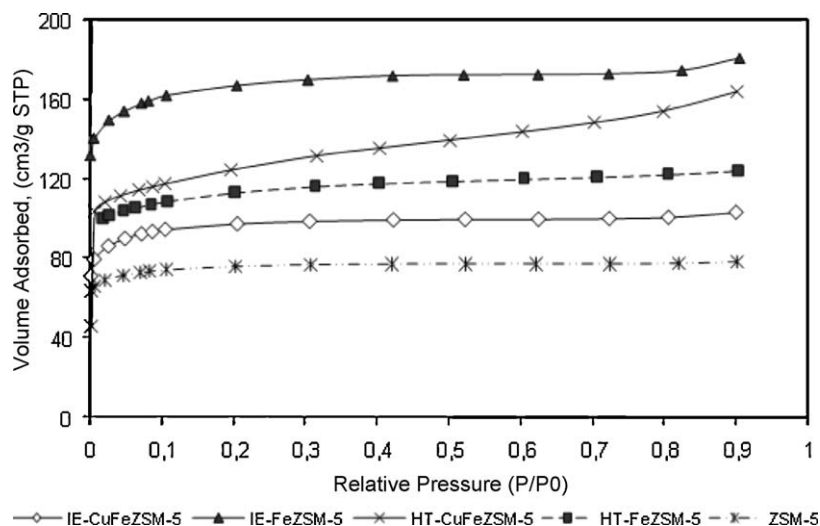


Fig. 5. Nitrogen adsorption isotherms of the samples.

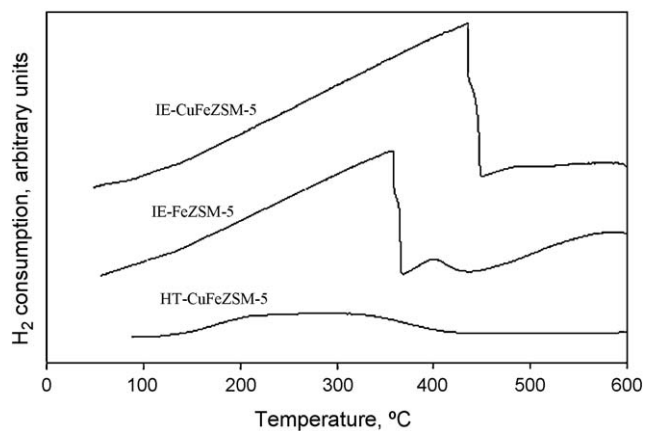


Fig. 6. Temperature-programmed reduction of catalysts: H<sub>2</sub> uptake of IE-FeZSM-5, IE-CuFeZSM-5 and HT-CuFeZSM-5.

### 3.7. Catalytic wet peroxide oxidation (CWPO) studies of Rhodamine 6G

Catalytic wet peroxide oxidation runs of Rhodamine 6G were carried using 150 cm<sup>3</sup> of 100 ppm (0.1 g/dm<sup>3</sup>) dye solution at a temperature of 323 K, for a catalyst amount of 0.15 g and H<sub>2</sub>O<sub>2</sub> amount of 40 mmol. The reaction duration was taken to be 2 h.

No noticeable dye removal by adsorption (blank run in the same conditions but without H<sub>2</sub>O<sub>2</sub>) took place during wet peroxide oxidation experiments for HT-CuFeZSM-5 catalyst while for IE-CuFeZSM-5 catalyst an aromatic content removal of 3.1% and a color removal of around 18% were measured.

The extent of decolorization and degradation of aqueous solution of R6G were determined as a function of time by measuring the absorbance values at 523 and 275 nm, respectively. Fig. 7 illustrates the change of absorbance at 523 nm as a function of time over HT-FeZSM-5 catalyst.

#### 3.7.1. Catalytic activities of different catalysts

The influence of catalyst preparation method on color removal and aromatic content removal as a function of time is presented in Fig. 8 for initial pH of 6–8. Parent zeolite (ZSM-5) had already some iron (0.64% in wt.). A color removal of 64.5% was noticed after a reaction time of 2 h when parent zeolite was used as catalyst, Fig. 8a. But no aromatic content removal was obtained with ZSM-5.

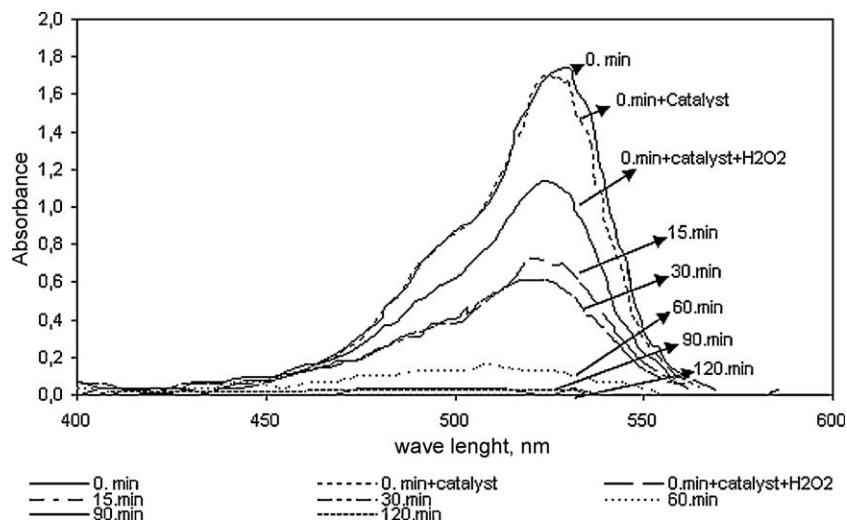
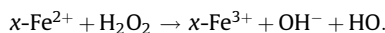


Fig. 7. The change of absorbance at 523 nm as a function of time over HT-FeZSM-5.

However, in iron and copper loaded ZSM-5 zeolite, IE-CuFeZSM-5, the color removal of about 100% was achieved after 1.5 h with an aromatic content removal of 53.2% after 2 h (Fig. 8b). The difference in catalytic activity between parent ZSM-5 and IE-CuFeZSM-5 samples can be attributed to well-dispersed iron and copper ions with a high concentration (19.54% iron and 2.53% copper) in the catalyst IE-CuFeZSM-5.

On the other hand, addition of catalyst and then H<sub>2</sub>O<sub>2</sub> to the reacting mixture increased the pH of the solution first for both the catalysts (Fig. 8c). This observation pointed out that some of Fe<sup>2+</sup> species present in zeolite structure are oxidized during the reaction:



where  $x$  presents the surface of the catalyst.

As the reaction proceeds, a sharp decrease in pH was observed with ZSM-5 while in the presence of IE-CuFeZSM-5 catalyst the pH of the solution remained almost constant after a slight decrease in pH. The decrease in pH might reflect the interaction between the basic dye molecules and the acidic surface of ZSM-5 zeolite. This interaction might be stronger for the parent ZSM-5 zeolite and due to the blocking of active sites, a lower color removal efficiency is obtained for this catalyst.

The catalyst prepared by ion-exchange method, IE-CuFeZSM-5, achieved complete color removal after 90 min of catalytic oxidation. This was followed by the catalyst prepared by hydrothermal treatment, HT-CuFeZSM-5 (99.0% removal after 2 h). The lowest decolorization extent was obtained with IE-FeZSM-5 catalyst without copper loading (27.6% after 2 h). This result might arise from the fine dispersion of iron in zeolite structure. The comparison of color removal extents obtained with IE-CuFeZSM-5 and IE-FeZSM-5 showed the importance of copper loading to FeZSM-5 zeolite.

The Si/Al ratio determines the number of Brönsted acid sites in ZSM-5 and therefore also the capacity to introduce copper and iron ions at exchangeable sites. In our case Si/Al ratio of parent ZSM-5 zeolite was low, 22. Therefore it has a high ion-exchange capacity. However, at high copper or iron concentrations aggregates of CuO and Fe oxide may be formed which are much less active than Cu<sup>2+</sup> and Fe<sup>2+</sup>. They may block the pores of ZSM-5, resulting in decreased activity [19,22]. The amount of copper and iron loaded into the catalyst was lower in the catalyst with hydrothermal treatment, HT-CuFeZSM-5, than that in the catalyst with ion

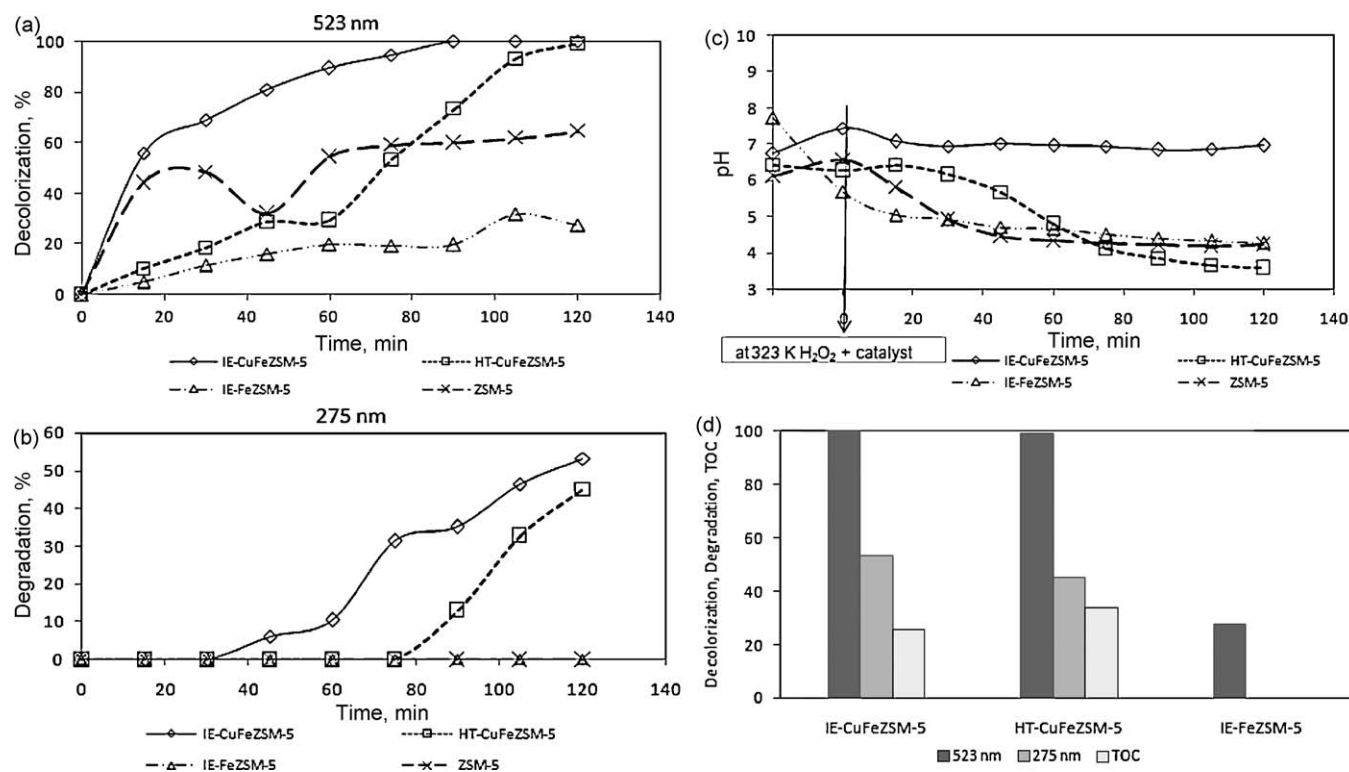


**Fig. 8.** The influence of catalyst type on color removal and aromatic content removal as a function of time for initial pH of 6–8. (a) Decolorization %, (b) degradation %, (c) pH value, (d) TOC % removal.

exchange, IE-CuFeZSM-5. The low copper and iron content revealed a decrease in catalytic activity of HT-CuFeZSM-5 catalyst.

The aromatic content removal at 275 nm followed also the similar trend with the highest removal of 53.2% for IE-CuFeZSM-5 and then 45.0% for HT-CuFeZSM-5 after an oxidation time of

2 h. No aromatic removal was achieved with IE-FeZSM-5 catalyst.

The destruction of a dye should be evaluated as an overall degradation process, involving the ultimate mineralization of both the parent dye and its intermediates which are produced during

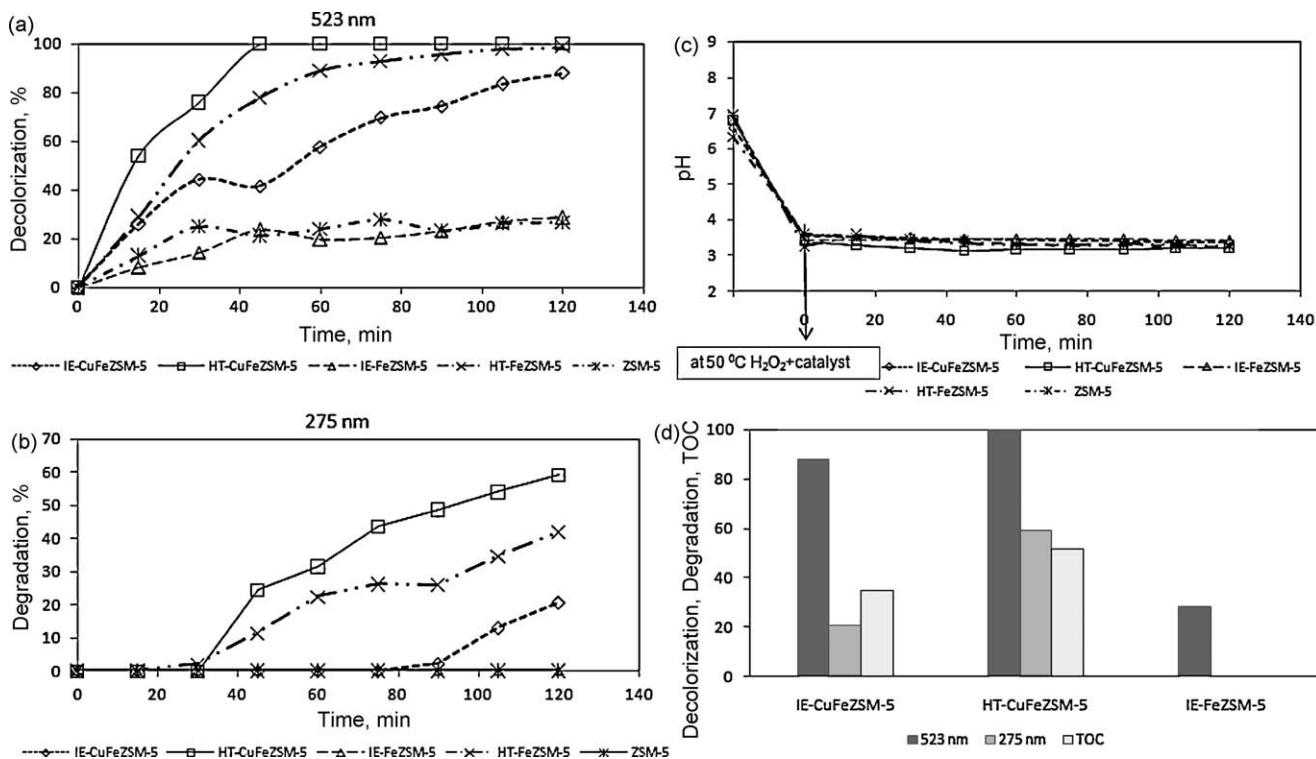


**Fig. 9.** The influence of preparation method of catalyst on color removal and aromatic content removal as a function of time for initial pH of 3–4. (a) Decolorization %, (b) degradation %, (c) pH value, (d) TOC % removal.

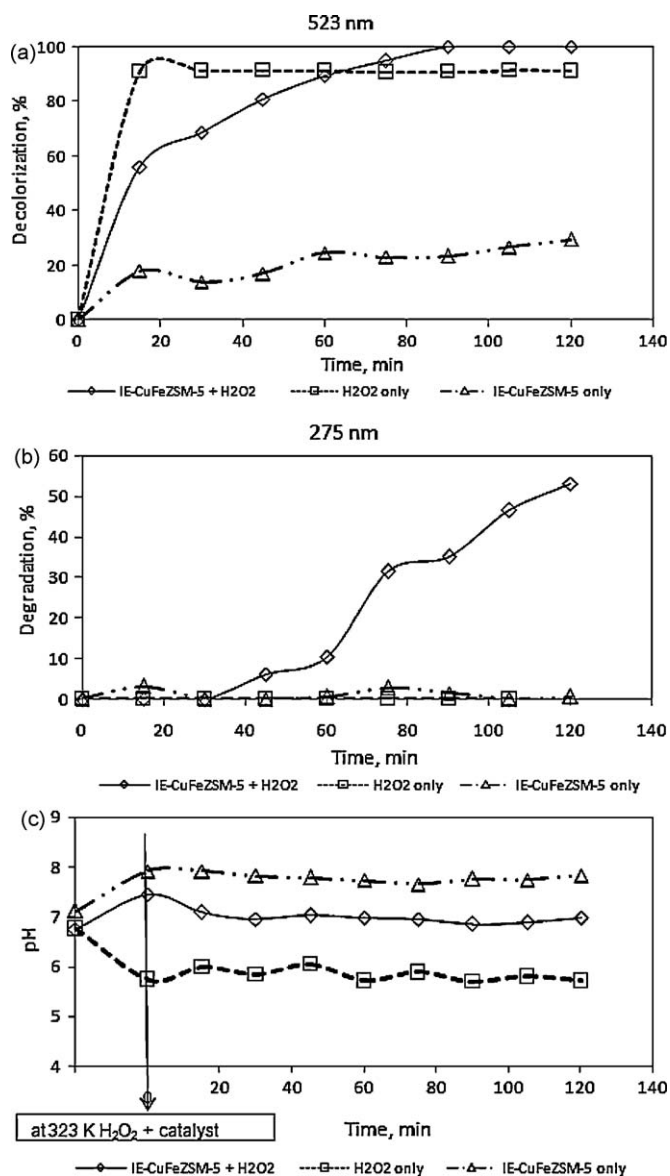


**Fig. 10.** The influence of H<sub>2</sub>O<sub>2</sub> in the oxidation of R6G for the catalyst of IE-CuFeZSM-5. (a) Decolorization %, (b) degradation %, (c) pH value.

the oxidative degradation process. The estimation of the overall process was done by monitoring the reduction of total organic carbon. Fig. 8d presents TOC elimination after a reaction time of 2 h for the catalysts tested at initial pH of 6–8. Reported TOC values represent the average of three measurements. It was found that the highest TOC removal was obtained by HT-CuFeZSM-5 as 34%. This was followed by a removal degree of 25.7% over IE-CuFeZSM-5. No TOC elimination was measured with IE-FeZSM-5 catalyst.

Fig. 9 presents the catalytic behavior of the catalysts for initial pH of 3–4 which was regulated by addition of H<sub>2</sub>SO<sub>4</sub> into the dye

solution. During the runs, after the regulation of pH, the solution pH remained constant at around a pH value of 3.5 (Fig. 9c). The following ordering was obtained for color removal efficiency of the catalysts after an oxidation time of 2 h: HT-CuFeZSM-5 > HT-FeZSM-5 > IE-CuFeZSM-5 > IE-FeZSM-5 ≈ ZSM-5. In contrast to the results at high initial pH value (6–8), catalyst prepared by hydrothermal treatment, HT-CuFeZSM-5, was the best for color removal. It had the highest initial color removal rate and complete color removal was achieved after 45 min. The positive influence of the presence of copper in FeZSM-5 zeolites was observed for both preparation methods, ion exchange and hydrothermal synthesis. The aromatic content removal measured was 59.1, 41.7 and 20.6% on catalysts HT-CuFeZSM-5, HT-FeZSM-5 and IE-CuFeZSM-5, respectively. However no aromatic content removal could be detected with IE-FeZSM-5 and ZSM-5 samples for initial pH of 3–4.

TOC elimination for the catalysts tested at initial pH of 3–4 was presented in Fig. 9d. Once again, TOC elimination on HT-CuFeZSM-5 was higher (51.8%) than that on IE-CuFeZSM-5 (34.5%). No TOC reduction was obtained with IE-FeZSM-5 catalyst. When Figs. 8d and 9d were compared it was noted that the decrease of initial pH from 6–8 to 3–4 enhanced the TOC removal for both catalysts, HT-CuFeZSM-5 and IE-CuFeZSM-5.

When the results displayed in Figs. 8 and 9 over IE-CuFeZSM-5 or HT-CuFeZSM-5 catalysts were compared at two initial pH values, it was seen that, the best values for the R6G degradation were obtained at initial pH = 6.7 for IE-CuFeZSM-5 catalyst (color removal 100% and aromatic content removal 53.2% after 2 h reaction time) and at pH = 3.4 for HT-CuFeZSM-5 catalyst (color removal 100% and aromatic content removal 59.1% after 2 h oxidation). Consequently, at high pH value, IE-CuFeZSM-5 was the most active catalyst for decolorization and degradation. However, at low pH value, HT-CuFeZSM-5 was the most active one.

Addition of H<sub>2</sub>O<sub>2</sub> to the reacting mixture caused an increase in pH of the solution because of the oxidation of some Fe<sup>2+</sup> species present in the zeolites.

The decreased performance at lower pHs for the IE-CuFeZSM-5 catalyst could be attributed to the inhibition of the reaction between Fe<sup>3+</sup> and H<sub>2</sub>O<sub>2</sub>, because the formation of the Fe<sup>3+</sup> peroxocomplexes (as intermediates) decreased with decreasing pH. On the other hand, the stability of H<sub>2</sub>O<sub>2</sub> was affected by the pH. A lower degree of decomposition was observed at pH values between 3 and 4 [1]. Above pH = 4, H<sub>2</sub>O<sub>2</sub> decomposes rapidly and molecular oxygen is produced without formation of significant amounts of hydroxyl radicals. In the presence of IE-CuFeZSM-5 catalyst, the pH value remained unchanged during the treatment when initial pH was 6.7. However, in the presence of HT-CuFeZSM-5 catalyst pH decreased from 6.4 (initial pH) to about 3.6 with the reaction time. This phenomenon could be explained by the fragmentation of the azo dye molecules into organic acids which led to a drop of pH. Similar trend in the change of pH of the reaction mixture was observed with IE-FeZSM-5 catalyst at an initial pH of 7.7 too (Fig. 8c). The catalytic performance of this catalyst was not affected by the reduction of solution pH to 3.4 with H<sub>2</sub>SO<sub>4</sub> addition. The color removal was measured to be about 28% for both initial pH values without aromatic content removal after a reaction time of 2 h, Figs. 8 and 9.

**Table 2**

Iron and copper leached during the CWPO reaction of R6G after 2 h of reaction.

Catalyst	Iron leached, mg/dm <sup>3</sup> , without pH regulation/with pH regulation	Iron loss, % without pH regulation/with pH regulation	Copper leached, mg/dm <sup>3</sup> without pH regulation/with pH regulation	Copper loss, % without pH regulation/with pH regulation
ZSM-5	–	–	–	–
IE-FeZSM-5	0.15/0.2	0.08/0.1	–/–	–/–
IE-CuFeZSM-5	0.5/0.4	0.25/0.2	12.3/13.7	48.4/53.7
HT-CuFeZSM-5	0.7/0.8	2.4/2.8	1.4/2.1	14.7/22.0

In addition to the experiments for the catalytic activity of IE-CuFeZSM-5 and HT-CuFeZSM-5 as catalysts in the CWPO of R6G in water, blank experiments were carried out for the systems (1) R6G and H<sub>2</sub>O<sub>2</sub> without any catalyst, (2) R6G and catalyst without H<sub>2</sub>O<sub>2</sub> under the same conditions of catalytic activity runs.

The influence of H<sub>2</sub>O<sub>2</sub> in the oxidation of R6G is displayed in Fig. 10 for IE-CuFeZSM-5 catalyst for initial pH of 6–8. In the presence of IE-CuFeZSM-5 catalyst alone in the solution, reaction was proceeded slowly and a low color removal (29.4%) was measured after a reaction time of 2 h. However, the introduction of H<sub>2</sub>O<sub>2</sub> into dye solution in the presence of catalyst led to an increase in the reaction rate as expected, because of the formation of the hydroxyl radicals. After a reaction duration of 90 min a complete color removal was achieved. However, when H<sub>2</sub>O<sub>2</sub> was present alone in the solution, the initial decolorization rate became higher than that in the presence of catalyst. But after 15 min of reaction, color removal efficiency remained constant at about 91%. An aromatic content removal at 275 nm was obtained only when the catalyst and H<sub>2</sub>O<sub>2</sub> were present together in the solution (53.2% after 2 h).

However, in the presence of HT-CuFeZSM-5 catalyst alone (without H<sub>2</sub>O<sub>2</sub>) neither color removal nor aromatic content removal was obtained at initial pH of 3.5. When HT-CuFeZSM-5 catalyst and H<sub>2</sub>O<sub>2</sub> were present together, color removal efficiency and aromatic removal were measured after 2 h to be 100 and 59.1%, respectively, Fig. 9.

### 3.7.2. Catalyst leaching tests

The evaluation of catalyst loss from a catalyst has a great importance in order to use it in industry. Amount of iron and copper loss into the solution was determined by measuring the iron and copper concentration in the solution after a reaction time of 2 h by atomic absorption spectrophotometer (Varian 10 plus). Table 2 presents iron and copper leached. Some important results must be stressed. First, in all cases iron leaching was considerably low (<1 mg/dm<sup>3</sup>, which was below the EU directives (<2 mg/dm<sup>3</sup>). The leaching of Fe and Cu cations from zeolite catalysts into the solution was dependent strongly on pH [1]. As expected, with the regulation of pH to about 3.5, iron leaching increased. Copper loss was more significant, especially for IE-CuFeZSM-5 catalyst. Copper leaching of IE-CuFeZSM-5 catalyst was about 7 times greater than that of HT-CuFeZSM-5 catalyst. It was noted that the latter one showed a good behavior in terms of degradation (45% at pH = 6.4, 59.1% at pH = 3.4), decolorization (99.0% at pH = 6.4, 100% after 45 min at pH = 3.4) and TOC removal (34% at pH = 6.4, 51.8% at pH = 3.5). For IE-CuFeZSM-5 catalyst, degradation, decolorization and TOC removal degrees were measured to be 53.2, 100 and 25.7% at pH 6.4 and 20.6, 41.5% (after 45 min) and 34.5% at pH 3.5. As seen HT-CuFeZSM-5 was a more active catalyst compared to IE-CuFeZSM-5 catalyst. Therefore, for long-term stability, it would be preferable to use this catalyst at pH of 6.4.

## 4. Conclusions

Fe and Cu containing ZSM-5 zeolites were prepared by ion exchange and by hydrothermal synthesis. Cu and iron were finely dispersed as extraframework ion and/or oxide species in catalysts prepared by ion-exchange method. Hydrothermally prepared HT-CuFeZSM-5 contained Fe and Cu in their framework. Leaching of extraframework ions and species was much larger than those in the framework. So Fe and Cu in the structural positions were more stabilized against leaching. It was revealed that both framework and extraframework Fe could catalyze the oxidation reaction of Rhodamine 6G in aqueous solution. However, the framework Fe

and Cu were found to be more active than extraframework. The presence of H<sub>2</sub>O<sub>2</sub> in the solution was found to have a major effect on decolorization and degradation.

## Acknowledgements

The authors acknowledge the financial support from TÜBİTAK (The Scientific and Technological Research Council of Turkey) and NASU (National Academy of Sciences of Ukraine) under project number 107M625.

This study is dedicated to the memory of Dr. M.V. Sychev (died in March 2009) who was the former director of Ukraine side for this joint project.

## References

- [1] R. Centi, S. Parathoner, T. Torre, M.G. Verduna, *Catalysis Today* 55 (2000) 61–69.
- [2] E. Guelue, J. Barrault, J. Fournier, J.-M. Tatibouet, *Applied Catalysis B: Environmental* 44 (2003) 1–8.
- [3] C. Wailling, *Accounts of Chemical Research* 8 (1975) 125–131.
- [4] M. Neamtu, C. Zaharia, C. Catrinescu, A. Yediler, M. Macoveanu, A. Ketrup, *Applied Catalysis B: Environmental* 48 (2004) 287–294.
- [5] M. Neamtu, A. Yediler, I. Siminiceanu, A. Ketrup, *Journal of Photochemistry and Photobiology A: Chemistry* 161 (2003) 87–93.
- [6] G. Bertanza, C. Collivignarelli, R. Pedrazzani, *Water Science Technology* 44 (2001) 109–116.
- [7] E.G. Solozhenko, N.M. Soboleva, V.V. Goncharuk, *Water Research* 29 (1995) 2206–2210.
- [8] S.F. Kang, H.M. Chang, *Water Science Technology* 36 (1997) 215–222.
- [9] J.H. Ramirez, C.A. Costa, L.M. Madeira, G. Mata, M.A. Vicente, M.L. Rojas-Cervantes, A.J. Lopez-Peinado, R.M. Martin-Aranda, *Applied Catalysis B: Environmental* 71 (2007) 44–56.
- [10] A.H. Gemeay, I.A. Mansour, R.G. El-Sharkawy, A.B. Zaki, *Journal of Molecular Catalysis A: Chemistry* 193 (2003) 109–120.
- [11] V.V. Ishtchenko, K.D. Huddersman, R.F. Vitkovskaya, *Applied Catalysis A: General* 242 (2003) 123–137.
- [12] S. Letaief, B. Casal, P. Aranda, M.A. Martín-Luengo, E. Ruiz-Hitzky, *Applied Clay Science* 22 (2003) 263–277.
- [13] G. Tachiev, J.A. Roth, A.R. Bowers, *International Journal of Chemical Kinetics* 32 (2000) 24–35.
- [14] F. Martínez, G. Calleja, J.A. Meleró, R. Molina, *Applied Catalysis B: Environmental* 60 (2005) 181–190.
- [15] K. Fajferberg, H. Debellefontaine, *Applied Catalysis B: Environmental* 10 (1996) L229–L235.
- [16] J. Barrault, C. Bouchoule, K. Echachoui, N. Frini-Srasra, M. Trabelsi, F. Bergaya, *Applied Catalysis B: Environmental* 15 (1998) 269–274.
- [17] K. Pirkanniami, M. Sillanpää, *Chemosphere* 48 (2002) 1047–1060.
- [18] A.V. Kucherov, A.N. Shigapov, A.V. Ivanov, T.N. Kucherova, L.M. Kustov, *Catalysis Today* 110 (2005) 330–338.
- [19] H.S. Jövall, L. Olsson, E. Fridell, R.J. Blint, *Applied Catalysis B: Environmental* 64 (2006) 180–188.
- [20] L. Olsson, H.S. Jövall, R.J. Blint, *Applied Catalysis B: Environmental* 81 (2008) 203–217.
- [21] S.A. Yashnik, Z.R. Ismagilov, V.F. Anufrienko, *Catalysis Today* 110 (2005) 310–322.
- [22] M. Schwidder, M.S. Kumar, K. Klementiev, M.M. Phol, A. Brückner, W. Grünert, *Journal of Catalysis* 231 (2005) 314–330.
- [23] R. Szostak, V. Nair, T.L. Thomas, *Journal of the Chemical Society Faraday Transactions* 83 (1987) 487–494.
- [24] I.V. Stolyarova, I.B. Kovban, R.V. Prikhod'ko, A.O. Kushko, M.V. Sychev, V.V. Goncharuk, *Russian Journal of Applied Chemistry* 80 (5) (2007) 746–753.
- [25] N.H. Phu, T.T.K. Hoa, N. Van Tan, H.V. Thang, P. Le Ha, *Applied Catalysis B: Environmental* 34 (2001) 267–275.
- [26] F. Heinrich, C. Schmidt, E. Löffler, M. Menzel, W. Grünert, *Journal of Catalysis* 212 (2002) 157–172.
- [27] M.M. Mohamed, I.O. Ali, N.A. Eissa, *Microporous and Mesoporous Materials* 87 (2005) 93–102.
- [28] Y. Cheng, L.-J. Wang, J.-S. Li, Y.-C. Yang, X.-Y. Sun, *Materials Letters* 59 (2005) 3247–3430.
- [29] C.P. Nicolaidis, *Applied Catalysis A: General* 185 (1999) 211–217.
- [30] M.S. Batista, M.A. Morales, E. Baggio-Saitovich, E.A. Urquieta-Gonzalez, *Hyperfine Interactions* 134 (2001) 161–166.
- [31] E.V. Kuznetsova, E.N. Savinov, L.A. Vostrikova, V.N. Parmon, *Applied Catalysis B: Environmental* 51 (2004) 165–170.
- [32] K. Klier, *Methane Oxidation Over Dual Redox Catalysts*, Final Report, Lehigh University, 1992.
- [33] I.O. Ali, *Materials Science and Engineering A* 459 (2007) 294–302.
- [34] M.M. Mohammed, *Journal of Colloid Interface Science* 265 (2003) 106–114.